Electronic Supplementary Material (ESI) for Sustainable Energy & Fuels.

Minimising the levelised cost of electricity for bifacial solar panel arrays using Bayesian optmisation

ESI – Electronic Supplementary Information

Peter Tillmann,[a,b‡] Klaus Jäger,[a,b‡] and Christiane Becker[a*].

October 29, 2019

S.1 Climate diagrams

Figure S.1 shows climate diagrams for (a) the Dallas/Fort Worth area with a humid subtropical climate (Cfa) and (b) Seattle. Depending on the source, the climate for Seattle is classified as warm temperate (Csb) or as oceanic (Cfb). Figure S.2 shows climate diagrams for (a) Daggett in the Mojave desert with a hot desert climate (BWh) (b) and Casa Blanca in Havana (Cuba) with a tropical climate (A).

S.2 Irradiance distribution

Figure S.3 shows the distribution of the global horizontal irradiance and the share of diffuse light over the course of the year after applying the Perez Model for Seattle, Dallas, Mojave Dessert and Havana.

S.3 Further results

Figure S.4 shows how much the different irradiation components contribute to the total energy yield for a bifacial module with $d = 10$ m module spacing and $\theta_m = 42°$ tilt in Seattle, Havana and the Mojave Dessert.

Figure S.5 shows the radiation yield for the Mohave Dessert and Havana for different module spacing and tilt angles.

[a] *Helmholtz-Zentrum Berlin für Materialien und Energie, Albert-Einstein-Straße 16, D-12489 Berlin.*
[b] *Zuse Institute Berlin, Takustraße 7, D-14195 Berlin.*
∗ Corresponding author; E-mail: christiane.becker@helmholtz-berlin.de.
‡ These authors contributed equally to this work.

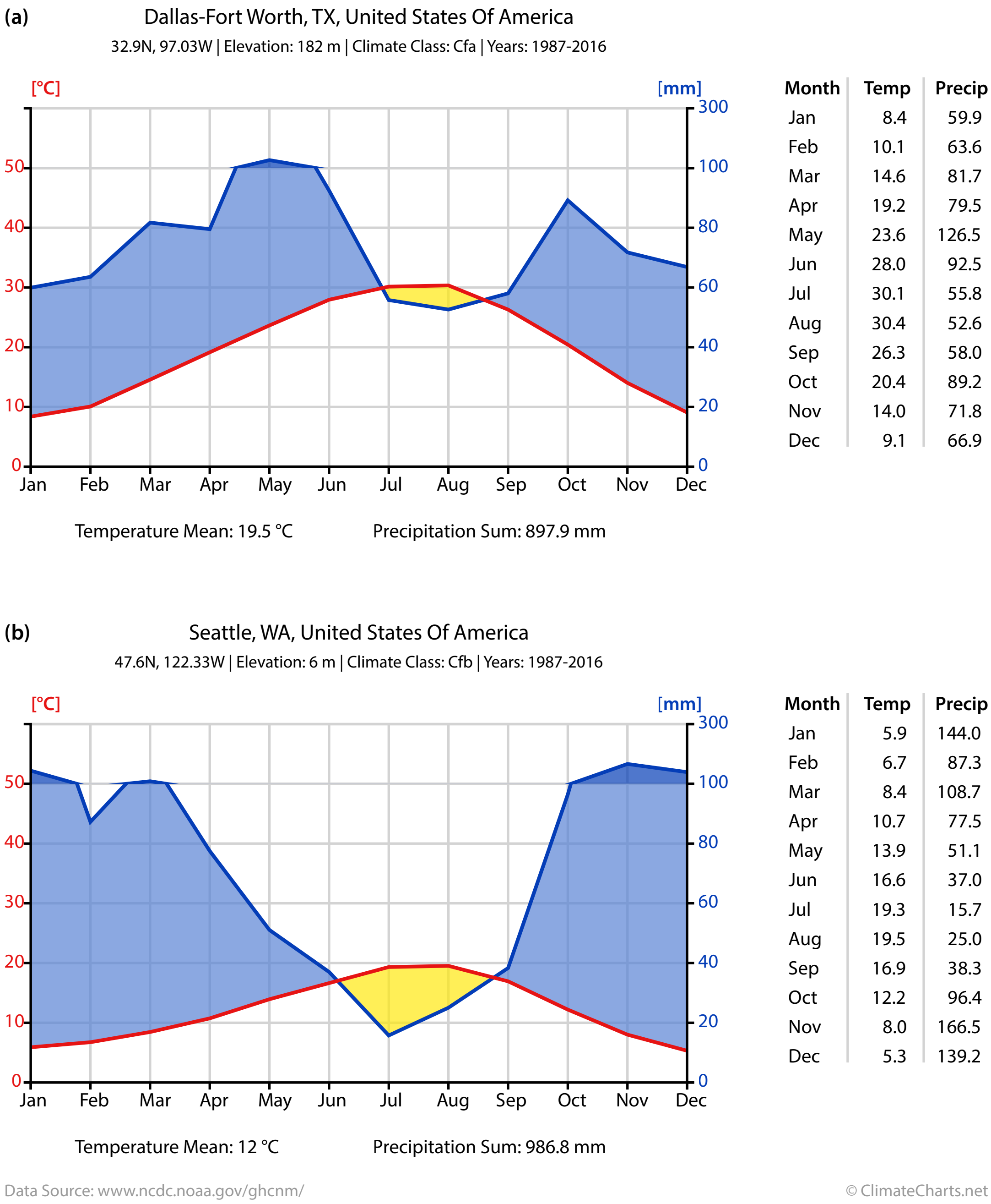

(a)

Month	Temp	Precip
Jan	8.4	59.9
Feb	10.1	63.6
Mar	14.6	81.7
Apr	19.2	79.5
May	23.6	126.5
Jun	28.0	92.5
Jul	30.1	55.8
Aug	30.4	52.6
Sep	26.3	58.0
Oct	20.4	89.2
Nov	14.0	71.8
Dec	9.1	66.9

(b)

Month	Temp	Precip
Jan	5.9	144.0
Feb	6.7	87.3
Mar	8.4	108.7
Apr	10.7	77.5
May	13.9	51.1
Jun	16.6	37.0
Jul	19.3	15.7
Aug	19.5	25.0
Sep	16.9	38.3
Oct	12.2	96.4
Nov	8.0	166.5
Dec	5.3	139.2

Figure S.1: Climate diagrams for (a) the Dallas/Fort Worth area and (b) Seattle. These charts were generated on `ClimateCharts.net` and are licensed under a Creative Commons Attribution 4.0 International License.

(a) Daggett/Faa Airport (Mojave desert), United States Of America

34.87N, 116.78W | Elevation: 585 m | Climate Class: BWh | Years: 1975-2004

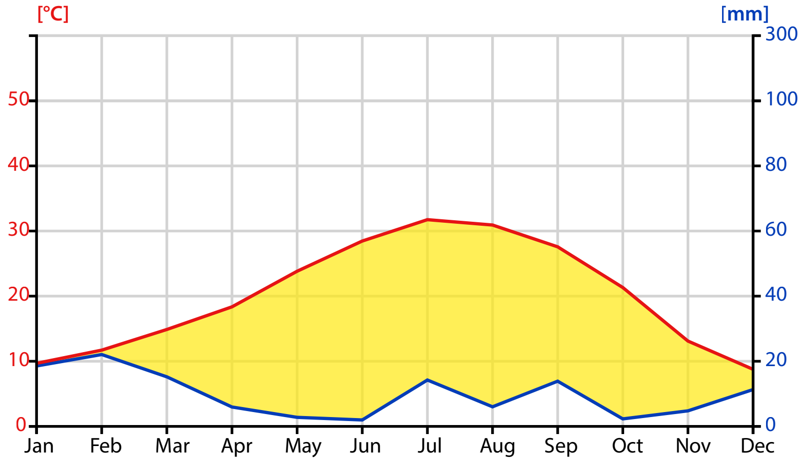

Month	Temp	Precip
Jan	9.7	18.6
Feb	11.7	22.1
Mar	14.9	15.2
Apr	18.4	5.9
May	23.8	2.8
Jun	28.5	2.0
Jul	31.7	14.2
Aug	30.9	6.0
Sep	27.6	13.9
Oct	21.3	2.3
Nov	13.1	4.8
Dec	8.8	11.3

Temperature Mean: 20.0 °C   Precipitation Sum: 119 mm

(b) Casa Blanca (Havana), Cuba

23.17N, 82.35W | Elevation: 50 m | Climate Class: A | Years: 1987-2016

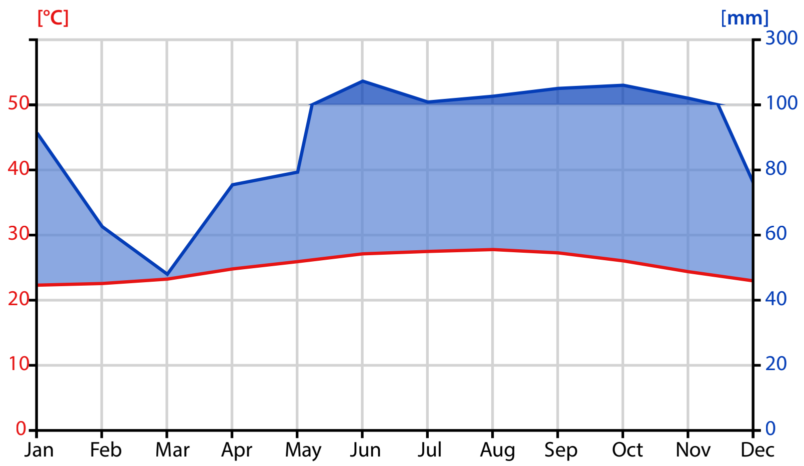

Month	Temp	Precip
Jan	22.3	91.4
Feb	22.6	62.6
Mar	23.2	48.0
Apr	24.8	75.4
May	25.9	79.3
Jun	27.1	172.8
Jul	27.5	108.6
Aug	27.8	126.4
Sep	27.3	150.4
Oct	26.0	160.1
Nov	24.4	120.2
Dec	23.0	75.9

Temperature Mean: 25.2 °C   Precipitation Sum: 1271.2 mm

Data Source: www.ncdc.noaa.gov/ghcnm/

Figure S.2: Climate diagrams for (a) Daggett in the Mojave desert and (b) Casa Blanca in Havana, Cuba. These charts were generated on `ClimateCharts.net` and are licensed under a Creative Commons Attribution 4.0 International License.

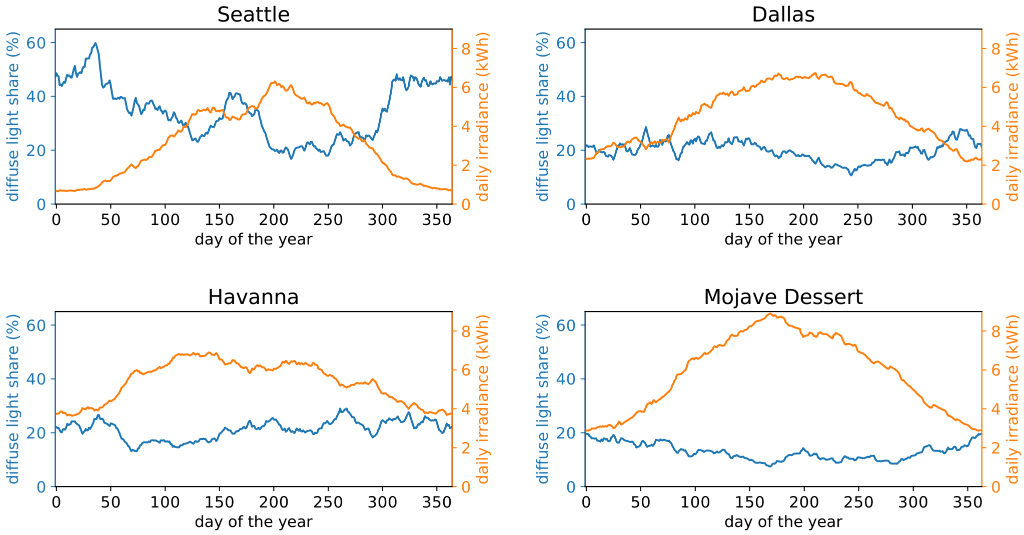

Figure S.3: 30 days moving average of isotropic diffuse light share (blue curve) and daily global horizontal irradiance (orange curve) for the typical meteorological year.

Figure S.7 and S.8 show the optimisation result for the Mojave Dessert and Havana respectively.

Figure S.6 compares the optimisation results for bifacial and monofacial solar cells for the Mojave Dessert and Havana.

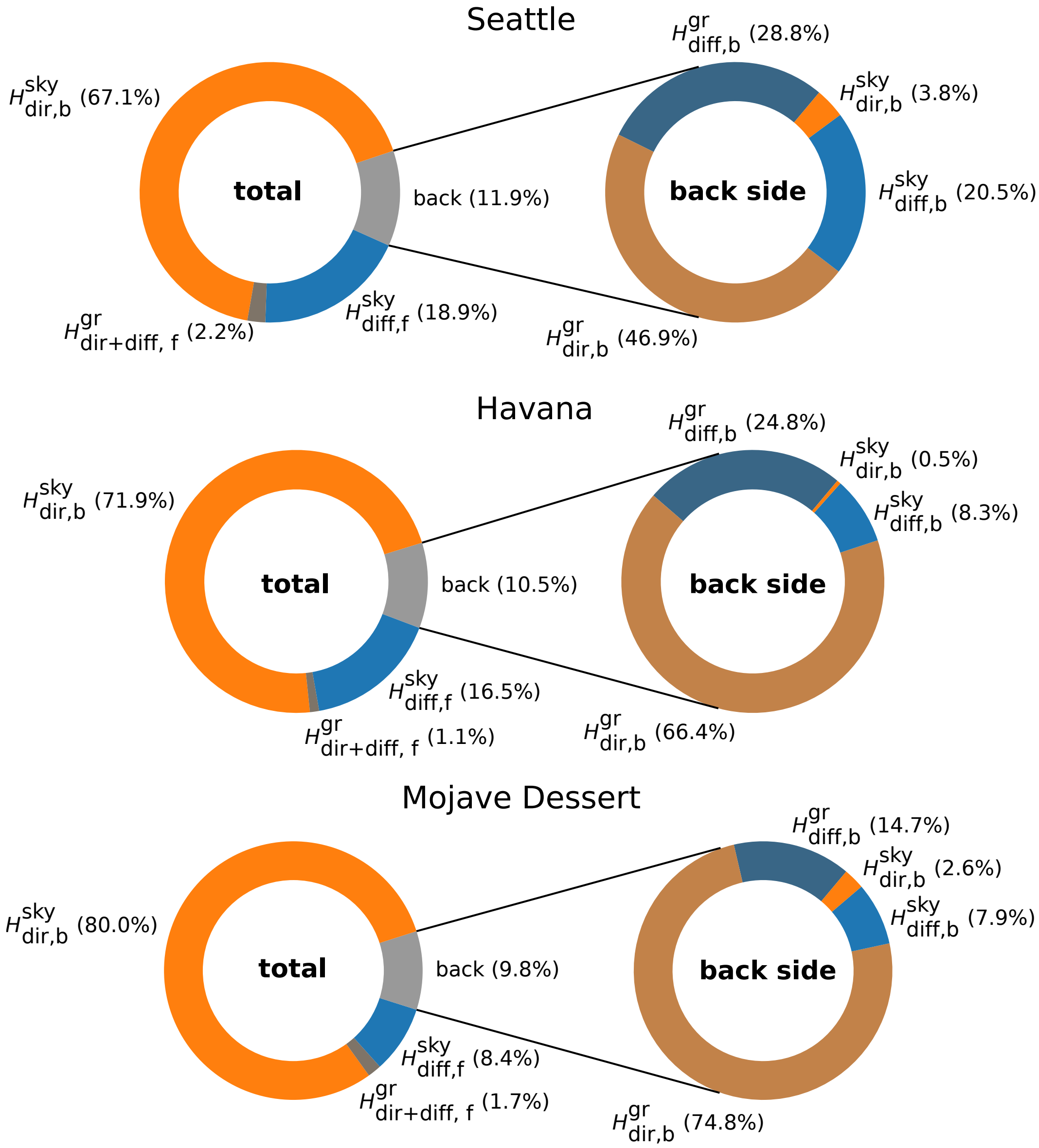

Figure S.4: (left) Different annual radiant exposure components for a bifacial solar cell in Seattle, Havanna and Mojave Dessert. (right) Detailed picture for the back side. Simulated with module spacing $d = 10$ m, module tilt $\theta_m = 42°$ m, module height $h = 0.5$ m and albedo $A = 30\%$.

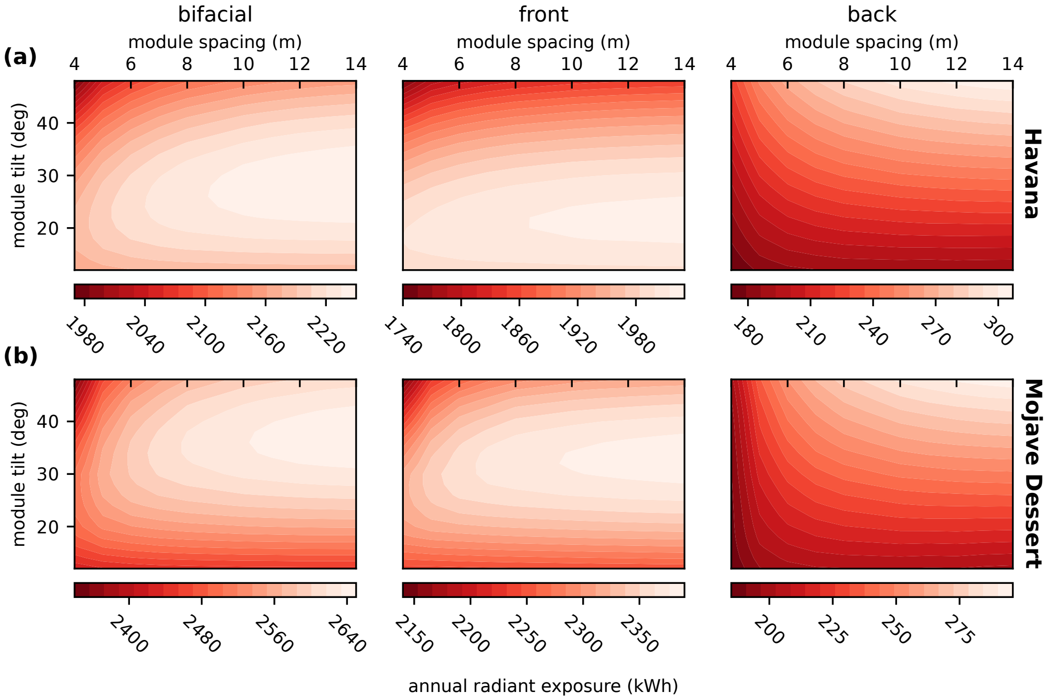

Figure S.5: Annual radiant exposure for bifacial modules and the contributions from front and back sides in a large PV field as a function of module spacing d and module tilt θ_m. Results are shown for Havana (top row) and Mojave Dessert (bottom row). The annual radiation yield is calculated using eq. (4) with $\eta_f = \eta_b = 1$. Simulated with m module height $h = 0.5$ m and albedo $A = 30\%$.

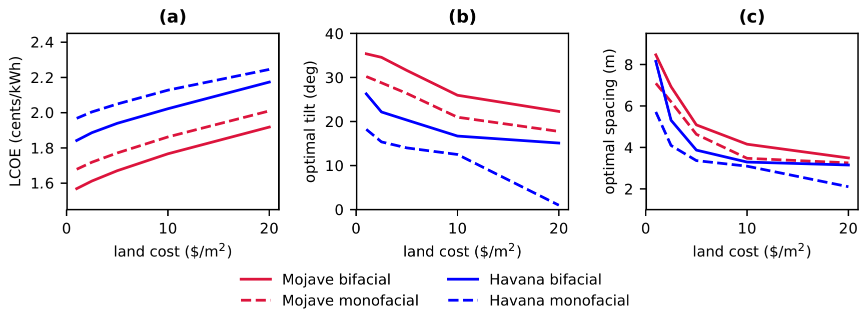

Figure S.6: Results of the optimisation for different land cost scenarios in Mojave Dessert (red lines) and Havana (blue lines): (a) lowest LCOE and (b) optimal module tilt and (c) optimal spacing. Simulations with albedo A = 30 %, module height h = 0.5 m and peak power costs c_p 1000 $/kWh.

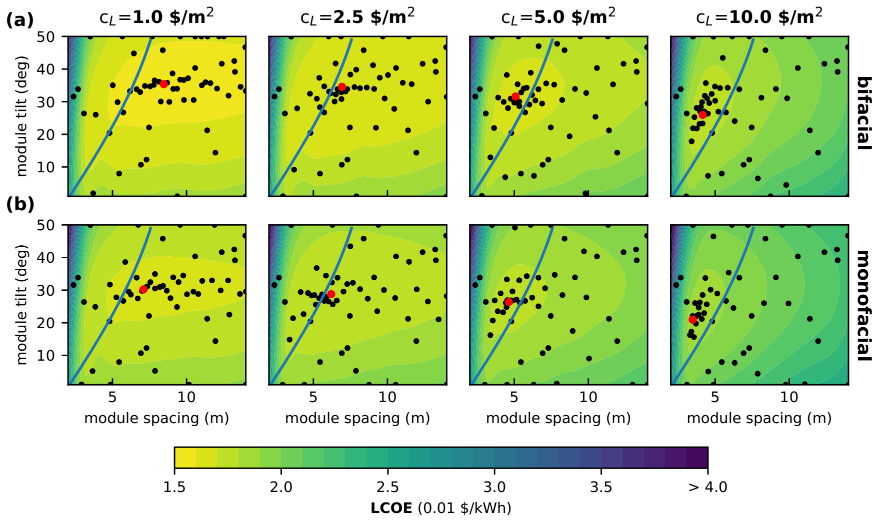

Figure S.7: Results of the Bayesian optimisation for minimising LCOE of (a) *bifacial* and (b) *monofacial* PV modules in the Mojave Dessert with the land cost c_L scenarios 1, 2.5, 5, and 10 $\$/m^2$. Black dots mark evaluated configurations and the color map corresponds to the interpolation by a Gaussian process. The red dot indicates the minimal LCOE. The blue curves indicate winter solstice rule. Simulations with albedo $A = 30$ %, module height $h = 0.5$ m and peak power costs $c_p = 1000$ $/kWh.

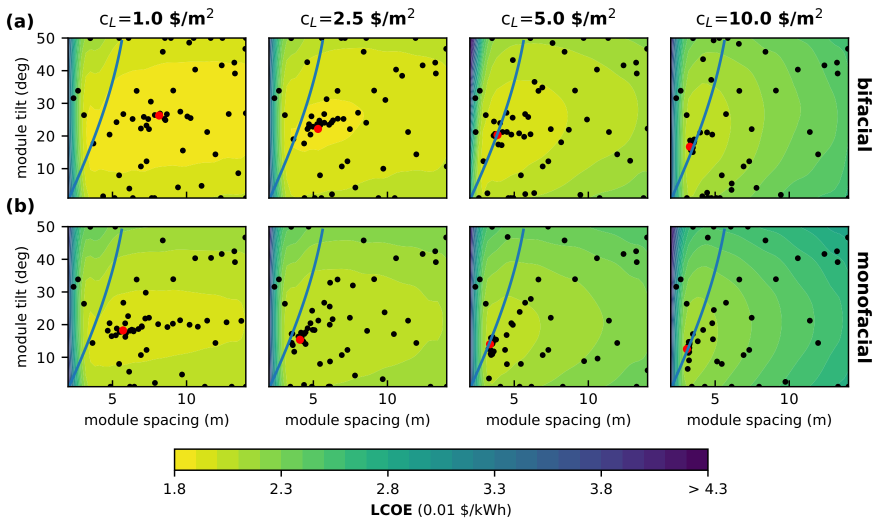

Figure S.8: Results of the Bayesian optimisation for minimising LCOE of (a) *bifacial* and (b) *monofacial* PV modules for Havana with the land cost c_L scenarios 1, 2.5, 5, and 10 $\$/m^2$. Black dots mark evaluated configurations and the color map corresponds to the interpolation by a Gaussian process. The red dot indicates the minimal LCOE. The blue curves indicate winter solstice rule. Simulations with albedo $A = 30$ %, module height $h = 0.5$ m and peak power costs $c_p = 1000$ $/kWh.